Initial-state effects in scanned-energy-mode photoelectron diffraction

V. Fritzsche
The Blackett Laboratory, Imperial College, London SW7 2BZ, United Kingdom

R. Davis, X.-M. Hu, and D. P. Woodruff
Physics Department, University of Warwick, Coventry CV4 7AL, United Kingdom

K.-U. Weiss, R. Dippel, K.-M. Schindler, Ph. Hofmann, and A. M. Bradshaw
Fritz-Haber-Institut der Max-Planck-Gesellschaft, Faradayweg 4-6, D-14195 Berlin (Dahlem), Germany
(Received 28 October 1993)

By a combination of experimental data [from the Ni(11$\bar{1}$)(2×2)-K structure], model calculations, and simple formal theory, it is shown that a strong initial-state effect exists in backscattering photoelectron diffraction, which can be ascribed to the parity of the emitted photoelectron source wave field. Unlike the initial-state effect recently discussed in forward scattering photoelectron (and Auger electron) diffraction, which is a spherical wave effect only present due to the close proximity of the emitter and scatterer, this parity effect in the backscattering geometry exists even in the lowest order approximation of the scattering, i.e., the plane wave approximation.

Photoelectron diffraction (see, e.g., Refs. 1–4) is primarily a final state effect; the structural information content of the measurements is a consequence of the interference of the elastically scattered and directly emitted components of the final photoelectron wave field. Nevertheless, there has been considerable interest recently in understanding the way that different source wave fields influence the observed photoelectron diffraction behavior.[5–15] Much of this recent work has concentrated on the forward (i.e., close to 0°) scattering geometry. The purpose of this paper is to demonstrate not only that initial state effects are also present in the backscattering geometry, but that they are actually far more important in this case. We show, in particular, that the source wave effects in forward scattering are second-order in nature, stemming entirely from the "curved wave" corrections to the scattering process, whereas in backscattering a first order effect is seen which can be readily understood in terms of the parity of the primarily emitted electron wave and the experimental geometry.

The recent work on initial state effects in the forward scattering geometry[8–10,12,13] has been undertaken mainly to clarify the different forward scattered angular distributions to be expected in photoelectron diffraction and Auger electron diffraction, and amplifies the earlier-established appreciation of the role of the angular momentum of the source wave in Auger electron diffraction.[16–19] The motivation for this has been to dispel misunderstandings[20–24] in the interpretation of some recent low energy Auger electron diffraction data. At high kinetic energies (typically above 500 eV), pronounced enhancements in the detected photoelectron or Auger electron intensities are seen in directions corresponding to forward scattering in a crystal surface, and can be readily attributed to constructive interference of the direct and scattered components of the electron wave field in this zero-order diffraction (i.e., an event in which the scattering pathlength difference is zero). This is the basis of the technique of XPD (x-ray photoelectron diffraction).[3,4] Of course, electron diffraction by atoms involves a phase shift, and if this phase shift were to be about π, even forward scattering would be destructive rather than constructive. At low energies (especially below about 100 eV) the phase of the complex scattering amplitude is often not small, and forward scattering destructive interference is possible. Under these conditions the angular momentum of the source wave plays a crucial role. Specifically, Terminello and Barton have measured the angular dependence of Cu $M_{2,3}M_{4,5}M_{4,5}$ Auger electron and Cu $3p$ photoemission from Cu(100) *at the same kinetic (final state) energy* and shown that they differ very significantly.[8] They have further shown that the difference can be understood in terms of the different dominant partial wave form of the unscattered source wave (mainly f-like and mixed s- and d-like, respectively).[12] The fact that these source waves lead to different scattering interferences is related to the close proximity of emitter and scattering atoms; for more distant scatterers this difference is lost.

In the scanned-energy mode photoelectron diffraction method, commonly referred to as PhD (Refs. 1 and 2) or ARPEFS (Ref. 25) (angle-resolved photoemission fine structure), photoemission from an adsorbate on a surface is measured as a function of photoelectron kinetic energy. The observed modulations in the intensity arise from the changing phase of backscattering events due to finite pathlength differences. A wide range of scattering angles may be involved, but if a single backscatterer lies directly behind the emitter relative to the detector (i.e., having a scattering angle of 180°), scattering from this atom typically dominates the observed periodicity of the PhD spectrum.[26,27] For such a scattering event, the *parity* of the source wave is crucial in determining whether the scattering event is constructive or destructive, as noticed already in Ref. 6. Consider, for example, photoemission from an s core state (i.e., one with the orbital

angular momentum quantum number $l = 0$). The optical selection rule allows only final states with $\Delta l = \pm 1$, so the outgoing unscattered photoelectron wave field is a p-wave directed along the polarization vector of the light. If we take the polarization vector to be in any direction other than perpendicular to the collection direction, then the odd parity of the p-wave means that the directly emitted component of the wave field, and that illuminating the 180° scatterer, have opposite sign; i.e., there is a phase difference of π. Consider now an initial p core state, which leads to an outgoing photoelectron wave which is a mixture of an s-wave and d-waves, all of even parity and thus having no phase difference between the direct and backscatterer illumination components. Clearly, the π phase difference between these two cases means that we expect constructive and destructive interference conditions to be totally inverted between these two different initial state conditions.

An example of this effect in experimental data[28] is shown in Fig. 1 in the form of PhD modulation spectra recorded in normal emission from the $2s$ and $2p$ core states of K adsorbed in a (2×2) phase on Ni(111); the K atom adsorbs atop outermost layer Ni atoms in this structure,[28–32] so this emission geometry corresponds to 180° scattering from the nearest neighbor Ni atom, although the detailed structure of both spectra is also influenced by scattering from other substrate atoms. What is clear, however, is that one spectrum is essentially the inverse of the other, confirming the importance of the different parities of the primary emitted electron waves.

In order to give a more rigorous account of this effect, and to compare it with the role of initial state effects in forward scattering, we now introduce some formal theory. The photoexcitation of a core state with angular momentum $L_i = (l_i, m_i)$ creates at the emitter atom an outgoing spherical electron wave, which is given by

$$\phi_f(\mathbf{r}) \propto \sum_L C_L(L_i) h_l(kr) Y_L(\hat{\mathbf{r}}). \tag{1}$$

If the polarization vector $\mathbf{u}$ is parallel to the z axis of the coordinate system, we obtain for the coefficients

$$C_L(L_i) = \sqrt{\frac{4\pi}{3}} e^{i\delta_l} \int dr r^3 R_l(r) \varphi_i(r) \times \int d\Omega_{\hat{\mathbf{r}}} Y_L^*(\hat{\mathbf{r}}) Y_{(1,0)}(\hat{\mathbf{r}}) Y_{L_i}(\hat{\mathbf{r}}), \tag{2}$$

where $\varphi_i(r)$ is the initial state wave function, $R_l(r)$ is a solution of the Schrödinger equation at the final state energy, and δ_l are the scattering phase shifts. Only coefficients with $l = l_i \pm 1$ and $m = m_i$ are nonzero.

If this source wave is then scattered at a neighboring atom, we obtain for the photoelectron intensity within the single scattering plane wave approximation

$$I(\mathbf{k}) \propto \sum_{m_i} \left| \sum_L C_L(L_i) i^{-l} Y_L(\hat{\mathbf{k}}) + \sum_L C_L(L_i) i^{-l} Y_L(\hat{\mathbf{R}}) \frac{e^{ikR - i\mathbf{k}\cdot\mathbf{R}}}{R} f(\hat{\mathbf{R}} \cdot \hat{\mathbf{k}}) \right|^2 . \tag{3}$$

Here, $\mathbf{R}$ is a vector between the emitter and a scattering atom, $f(\cos\Theta)$ is the scattering amplitude, $\hat{\mathbf{k}}$ is the unit vector pointing towards the detector, and k is the wave number ($\mathbf{k} = k\hat{\mathbf{k}}$). The intensity of the source wave alone,

$$I_0(\mathbf{k}) = \sum_{m_i} \left| \sum_L C_L(L_i) i^{-l} Y_L(\hat{\mathbf{k}}) \right|^2 , \tag{4}$$

depends only weakly on the energy due to the radial matrix elements in Eq. (2). The essential oscillations, observed in the PhD spectrum, arise from the mixed quadratic terms in Eq. (3):

$$I_1(\mathbf{k}) = \sum_{m_i} \sum_{L'} C_{L'}^*(L_i) i^{l'} Y_{L'}^*(\hat{\mathbf{k}}) \times \sum_L C_L(L_i) i^{-l} Y_L(\hat{\mathbf{R}}) \frac{e^{ikR - i\mathbf{k}\cdot\mathbf{R}}}{R} f(\hat{\mathbf{R}} \cdot \hat{\mathbf{k}}) + \text{c.c.} \tag{5}$$

This term contains l-dependent prefactors which are responsible for the observed phase shift between the $2s$ and $2p$ spectra in Fig. 1. In the 180° backscattering direction (i.e., for $\hat{\mathbf{R}} = -\hat{\mathbf{k}}$), we obtain by using $Y_L(-\hat{\mathbf{k}}) = (-1)^l Y_L(\hat{\mathbf{k}})$

$$I_1(\mathbf{k}) = (-1)^{l_i+1} I_0(\mathbf{k}) \frac{e^{ikR - i\mathbf{k}\cdot\mathbf{R}}}{R} f(\hat{\mathbf{R}} \cdot \hat{\mathbf{k}}) + \text{c.c.} \tag{6}$$

This means that the phase of the oscillations relative to the intensity of the primary wave is determined by the parity of the source wave. Of course, this treatment is not exact, and this simple conclusion relies on the conditions applied to the above derivation. Spherical wave corrections and the third term in the intensity [the absolute square of the scattered wave in Eq. (3)] give rise to small deviations from the general behavior described by Eq. (6) for a single backscattering atom. Moreover, the situation is more complicated for other scattering angles for which the orientation of the polarization vector comes into play explicitly. Nevertheless, the experimen-

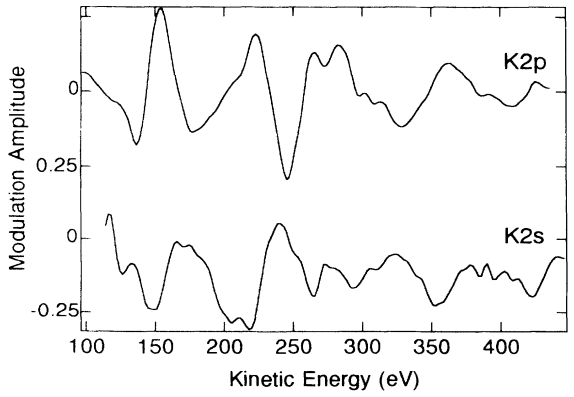

FIG. 1. K $2s$ and K $2p$ experimental PhD spectra recorded at normal emission from a Ni(111)(2×2)-K surface. Details of the experiment are given in Ref. 28.

tal spectra in Fig. 1 show that the parity effect for the near-backscattering events is strong enough to dominate over other single and multiple scattering contributions to the spectra.

A somewhat clearer view of the main effects in more general geometries can be obtained from the results of a series of simple single scattering calculations from individual atoms in different positions (Fig. 2). Figures 3–6 show such calculated spectra; in all cases the detector axis, the polarization vector, and the emitter-scatterer vector **R** lie in the same plane. The angle between polarization vector **u** and detector is 30° in all cases, as in the experiment which produced Fig. 1 (Ref. 28). The emitter is a K atom, the scatterer a Ni atom, and the distance between them is $R = 2.87$ Å as determined for the nearest neighbors in the Ni(111)(2×2)-K structure.[28] The angle between the polarization vector **u** and the interatomic distance **R** is denoted by ε. The s source wave is, of course, independent of ε and these spectra can be considered to be a reference for polarization-induced phase shifts. The single scattering spectra have been calculated with an exact spherical wave theory.[33] The radial matrix elements in Eq. (2) have been chosen such that the primary emitted electron wave is either a pure s, p, or d state. The period of the PhD oscillations in the calculated spectra increases as the scattering angle Θ decreases due to the argument $ikR(1 - \cos\Theta)$ in the phase factor in Eq. (3), which describes the effect of the scattering pathlength difference.

The underlying effect which we have described and which is confirmed by the experimental results is shown clearly in Fig. 3, which shows the effect of pure s, p, and d source wave scattering through an angle of 180° with $\varepsilon = 150°$, precisely the geometry of the nearest neighbor Ni scatterer in the experiment (position 1, Fig. 2). The parity-induced phase shifts of π are very clear. Figure 4 shows similar results for a scattering angle of 150° but

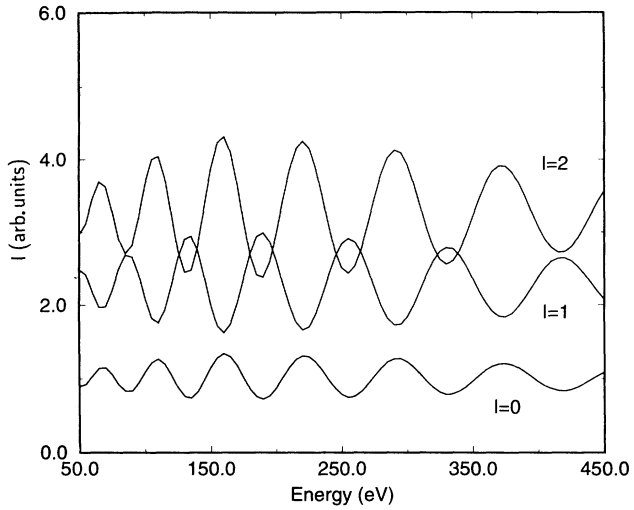

FIG. 3. Results of a spherical wave scattering calculation from a single Ni scatterer placed 2.87 Å below the emitter [i.e., the nearest neighbor scattering geometry appropriate to the Ni(111)(2×2)-K structure] with different angular momenta of the emitted electron, $\Theta = 180°$ and $\varepsilon = 150°$ (position 1 in Fig. 2).

two different values, 120° and 180° for ε (positions 2 and 2′, Fig. 2). The parity effect remains, but the modulation amplitudes are smaller than in Fig. 3 because the modulus of the scattering factor has a maximum for $\Theta = 180°$; there are amplitude changes between the two pairs of p and d spectra in Fig. 4 determined simply by the changing amplitude of illumination of the scatterer, which is largest for $\varepsilon = 180°$.

The situation becomes more complex for Ni atoms in positions 3 and 4, shown in Figs. 5 and 6, for which the smaller scattering angles (120° and 90°, respectively) mean that both the relative phase and amplitude of the

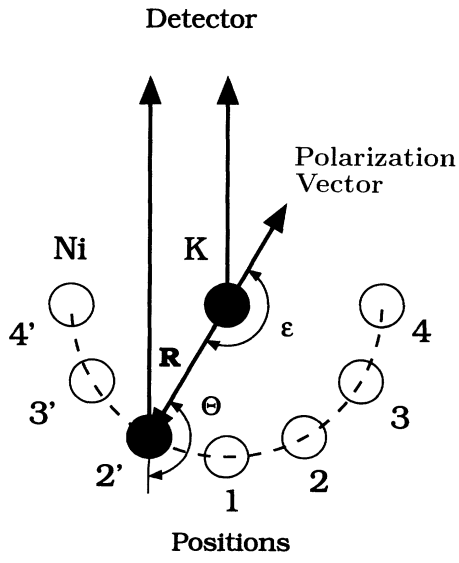

FIG. 2. Geometry for the single scattering calculations. The positions of the Ni scatterer for the spectra shown in Figs. 3–6 are indicated.

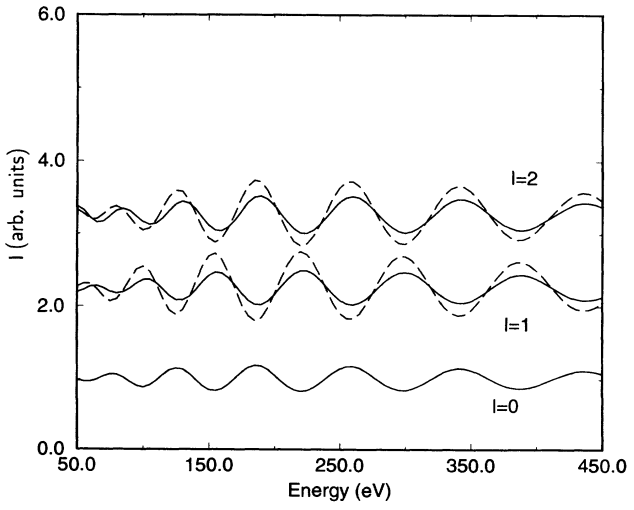

FIG. 4. Results of single scattering calculations as in Fig. 3 but with $\Theta = 150°$ and with $\varepsilon = 120°$ (solid lines, position 2) or $\varepsilon = 180°$ (dashed lines, position 2′).

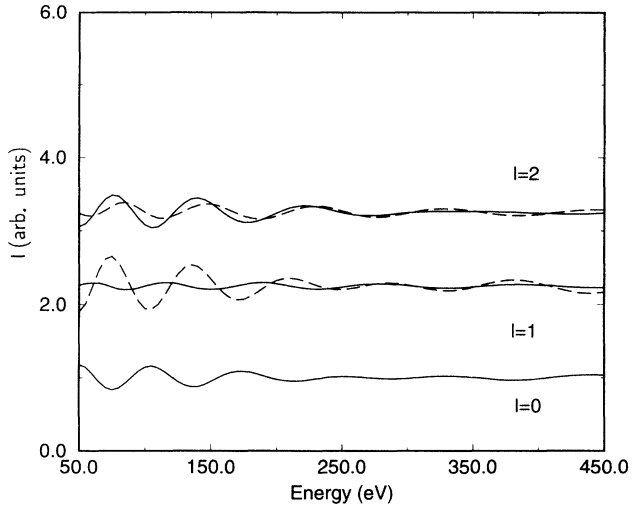

FIG. 5. Results of single scattering calculations as in Fig. 3 but with $\Theta = 120°$ and with $\varepsilon = 90°$ (solid lines, position 3) or $\varepsilon = 150°$ (dashed lines, position 3′).

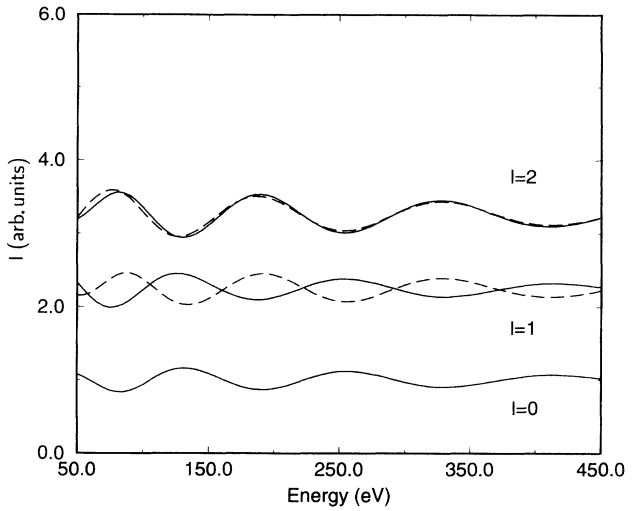

FIG. 6. Results of single scattering calculations as in Fig. 3 but with $\Theta = 90°$ and with $\varepsilon = 60°$ (solid lines, position 4) or $\varepsilon = 120°$ (dashed lines, position 4′).

direct and illumination waves depend on the exact location of the polarization vector relative to the interatomic vector **R**. In Fig. 5, the weakness of the modulations above 200 eV can be attributed to the small scattering amplitude for this special scattering angle. Notice that in Fig. 6 there is a phase shift of π in the p state PhD intensities between the two different positions of the atom, since a replacement of **R** by $-\mathbf{R}$ in Eq. (3) gives a prefactor of -1 in front of the scattered wave. By contrast, the two d state curves of Fig. 6 are in phase, since $Y_L(\hat{\mathbf{R}}) = Y_L(-\hat{\mathbf{R}})$ for $l = 2$. The slight deviations implied by these descriptions, which can be seen in Fig. 6, are caused by spherical wave effects, neglected in the plane wave approximation of Eq. (3), but included in the calculations.

In conclusion, we have shown both the experimental evidence for, and the origins of, a simple (and important) parity effect in the influence of the source wave on backscattering photoelectron diffraction. This effect is seen in the lowest order approximation (plane wave approximation) for all distances between emitter and scatterer, and contrasts with the much more subtle spherical wave effect which accounts for the initial state dependence in forward scattering photoelectron diffraction. One interesting implication of this result is that if the form of an emitted source wave field is in doubt (as it may be in some Auger electron emission experiments), backscattering diffraction may be a far more sensitive means to investigate this than angle-scan photoelectron diffraction.

The authors are pleased to acknowledge financial support from the German Federal Ministry of Research and Technology under Contract No. 05-5EB-FXB 2, the British Science and Engineering Research Council, as well as the Large Scale Installation and SCIENCE programmes of the European Community.

[1] D. P. Woodruff, in *Angle-Resolved Photoemission: Theory and Current Applications*, edited by S. D. Kevan (Elsevier, Amsterdam, 1992), p. 243.
[2] A. M. Bradshaw and D. P. Woodruff, in *Applications of Synchrotron Radiation: High Resolution Studies of Molecules and Molecular Adsorbates on Surfaces*, edited by W. Eberhardt (Springer-Verlag, Berlin, in press).
[3] C. S. Fadley, in *Synchrotron Radiation Research: Advances in Surface and Interface Science*, edited by R. Z. Bachrach (Plenum Press, New York, 1992).
[4] S. A. Chambers, Adv. Phys. **40**, 357 (1991).
[5] D. E. Parry, J. Electron Spectrosc. Relat. Phenom. **49**, 23 (1989).
[6] D. J. Friedman and C. S. Fadley, J. Electron Spectrosc. Relat. Phenom. **51**, 689 (1990).
[7] A. P. Kaduwela, D. J. Friedman, and C. S. Fadley, J. Electron Spectrosc. Relat. Phenom. **57**, 223 (1991).
[8] L. J. Terminello and J. J. Barton, Science **251**, 1218 (1991).
[9] Y. U. Idzerda and D. E. Ramaker, Phys. Rev. Lett. **69**, 1943 (1992).
[10] T. Greber, J. Osterwalder, D. Naumović, A. Stuck, S. Hüfner, and L. Schlapbach, Phys. Rev. Lett. **69**, 1947 (1992).
[11] D. K. Saldin, G. R. Harp, and B. P. Tonner, Phys. Rev. B **45**, 9629 (1992).
[12] J. J. Barton and L. J. Terminello, Phys. Rev. B **46**, 13 548 (1992).
[13] L. J. Terminello and J. J. Barton, Phys. Rev. B **47**, 6851 (1993).
[14] G. S. Herman, T. T. Tran, K. Higashiyama, and

C. S. Fadley, Phys. Rev. Lett. **68**, 1204 (1992).
[15] L. E. Klebanoff and D. G. Van Campen, Phys. Rev. Lett. **69**, 196 (1992).
[16] R. N. Lindsay and C. G. Kinniburgh, Surf. Sci. **63**, 162 (1977).
[17] H. L. Davis, in *Proceedings of the 7th International Vacuum Congress and 3rd International Conference on Solid Surfaces, Vienna, 1977*, edited by R. Dobrozemsky (Dobrozemsky, Vienna, 1977), p. 2281.
[18] D. Aberdam, R. Baudoing, E. Blanc, and C. Gaubert, Surf. Sci. **71**, 279 (1978).
[19] J. M. Plociennik, A. Barbet, and L. Mathey, Surf. Sci. **102**, 282 (1981).
[20] D. G. Frank, N. Batina, T. Golden, F. Lu, and A. T. Hubbard, Science **247**, 182 (1990).
[21] S. A. Chambers, Science **248**, 1129 (1990).
[22] W. F. Egelhoff, Jr., J. W. Gadzuk, C. J. Powell, and M. A. Van Hove, Science **248**, 1129 (1990).
[23] X. D. Wang, Z. L. Han, B. P. Tonner, Y. Chen, and S. Y. Tong, Science **248**, 1129 (1990).
[24] D. P. Woodruff, Science **248**, 1131 (1990).
[25] J. J. Barton, C. C. Bahr, Z. Hussain, S. W. Robey, J. G. Tobin, L. E. Klebanoff, and D. A. Shirley, Phys. Rev. Lett. **51**, 272 (1983).
[26] V. Fritzsche and D. P. Woodruff, Phys. Rev. B **46**, 16 128 (1992).
[27] K.-M. Schindler, Ph. Hofmann, V. Fritzsche, S. Bao, S. Kulkarni, A. M. Bradshaw, and D. P. Woodruff, Phys. Rev. Lett. **71**, 2054 (1993).
[28] R. Davis, X.-M. Hu, D. P. Woodruff, K.-U. Weiss, R. Dippel, K.-M. Schindler, Ph. Hofmann, V. Fritzsche, and A. M. Bradshaw, Surf. Sci. (to be published).
[29] D. Fisher, S. Chandavarkar, I. R. Collins, R. D. Diehl, P. Kaukasoina, and M. Lindroos, Phys. Rev. Lett. **68**, 2786 (1992).
[30] P. Kaukasoina, M. Lindroos, R. D. Diehl, D. Fisher, S. Chandavarkar, and I. R. Collins, J. Phys. Condens. Matter **5**, 2875 (1993).
[31] Zhengqing Huang, L. Q. Wang, A. E. Schach von Wittenau, Z. Hussain, and D. A. Shirley, Phys. Rev. B **47**, 13 626 (1993).
[32] D. L. Adler, I. R. Collins, X. Liang, S. Murray, G. S. Leatherman, K.-D. Tsuei, S. Chandavarkar, R. McGrath, R. D. Diehl, and P. H. Citrin (unpublished).
[33] V. Fritzsche, J. Phys. Condens. Matter **2**, 9735 (1990).